Third Joint Eurohaptics Conference and Symposium on Haptic Interfaces
for Virtual Environment and Teleoperator Systems
Salt Lake City, UT, USA, March 18-20, 2009

3-D Force Control on the Human Fingerpad Using a Magnetic Levitation Device for Fingernail Imaging Calibration

Thomas Grieve *
Department of Mechanical Engineering
University of Utah

Yu Sun†
School of Computing
University of Utah

John M. Hollerbach‡
School of Computing
University of Utah

Stephen A. Mascaro§
Department of Mechanical Engineering
University of Utah

ABSTRACT

This paper demonstrates fast, accurate, and stable force control in three axes simultaneously when a flat surface is pressed against the human fingerpad. The primary application of this force control is for the automated calibration of a fingernail imaging system, where video images of the human fingernail are used to predict the normal and shear forces that occur when the fingerpad is pressed against a flat surface.

The system consists of a six degree-of-freedom magnetic levitation device (MLD), whose flotor has been modified to apply forces to the human fingerpad, which is resting in a passive restraint. The system is capable of taking simultaneous steps in normal force and two axes of shear forces with a settling time of less than 0.2 seconds, and achieves a steady-state error as small as 0.05 N in all three axes. The system is also capable of tracking error of less than 0.2 N when the shear force vector rotates with a frequency of 1 rad/s. This paper also demonstrates the successful tracking of a desired force trajectory in three dimensions for calibrating a fingernail imaging system.

1 INTRODUCTION

The idea of "fingernail sensing" was first introduced by Mascaro and Asada [9] as a means of estimating forces at the human fingerpad by measuring the change in "coloration" of the fingernail that occurs when the finger is pressed against a surface. This was accomplished by instrumenting the fingernail with arrays of light-emitting diodes and photodetectors, enabling the fingernail sensors to detect the variations in capillary blood volume in the fingernail bed when force is applied to the fingerpad, not only in the normal direction, but also in the two shear directions. The sensor predicted normal force to within 1 N accuracy in the range of 0 to 3 N and shear force to within 0.5 N accuracy in the range of ± 2 N [11]. Mascaro and Asada later showed that common patterns of fingernail coloration occur across all people in response to fingernail force [10], justifying the broad utility of fingernail sensing, as well as suggesting future work in developing a common physically-based model of the coloration that could be tuned to each person. Potential applications for such unobtrusive finger force measurement include development of wearable human-computer interfaces such as mice and keyboards, as well as use as a tool for studying human grasping forces in real environments.

This original approach had two main limitations. One was the problem of getting the sensor to adhere firmly to the fingernail, which was only partially overcome by custom manufacturing of the sensor according to the shape of the fingernail of each individual user. Secondly, the original fingernail sensor only contained up to 6 or 8 detectors, making it somewhat equivalent to imaging the fingernail with a 6 or 8 pixel camera. As an alternative, Mascaro, Sun, and Hollerbach proposed the idea of "fingernail imaging" using a high resolution video camera [15, 16], which provides a much richer set of data while eliminating the need for customized manufacturing. Using the fingernail imaging technique, we were able to predict normal and shear forces to within 0.3 N accuracy in a range of 10 N [15]. Limitations of the fingernail imaging approach include the need to maintain line of sight with the camera, dealing with variable lighting conditions, and the increased computational burden associated with the image processing.

Both the fingernail sensing and fingernail imaging techniques have a common challenge, which is efficient and effective calibration of the mathematical models used to predict 3-axis forces. In order to generate a model that is capable of predicting forces over a range of combinations of normal and shear forces, a rich set of training data must be collected over the entire feasible portion of the 3D force space. In the past, we had to rely on the human subjects to apply the forces themselves using visual feedback from a 3-axis force sensor placed under the fingerpad. In [11], a graphical user interface was developed to prompt the subject to fully explore the feasible 3D force space by visually overlaying actual and desired forces in three dimensions. Since the display itself was only 2 dimensional, the two axes of shear forces were represented by the x-y coordinates of the center of a small circle, while the normal force was presented using the color of the circle. Later in [15], it was determined that varying the radius of the circle was a more effective presentation of normal force rather than varying color. In either case, it is still a difficult task for the human subject to control three variables simultaneously using 2D visual feedback. It is also fatiguing for the human subject to apply forces for an extended amount of time, especially for repeated training sessions. In order to minimize the fatigue in [11], a circling/spiraling training trajectory was devised to cover the feasible force space in a minimum amount of time. Because the trajectory follows a pattern, it induces a certain bias into the training data. When the models trained on these spiraling data sets were validated using new random force combinations, the performance of the models decreased significantly [11]. If the training data were composed from a random trajectory through the force space, it would take much longer to cover the force space, and the human subject would be even more fatigued. Finally, if we were to consider adding additional variables to the training session, such as varying the angles of contact of the finger with the surface, it would become totally impractical to rely on the human to control more than 3 variables simultaneously.

To overcome these problems, this paper introduces the use of an automated robotic system to apply three-axis forces to the human fingerpad in a controlled manner while the finger is resting in a passive restraint. Such a system needs to be able to perform 3-axis force control with speed, accuracy, and stability, while ensuring the safety of the human subject. Therefore we have chosen to use a 6 DOF magnetic levitation device (MLD) designed by Hollis [1]. This device was designed to provide haptic feedback through a joy-

*e-mail:tom.grieve@utah.edu
†e-mail:ysun@cs.utah.edu
‡e-mail: jmh@cs.utah.edu
§e-mail:smascaro@mech.utah.edu

stick that is grasped by the human hand. Instead, we modify the end-effector to apply forces to the fingerpad using a flat surface. This device has a well-suited range of positions and forces for our application, and is safe to use on a human finger, since the end-effector (flotor) is floating on magnetic fields that are incapable of generating forces large enough to hurt the finger.

The main purpose of this paper is to demonstrate successful three-axis force control and force tracking on the human fingerpad using the MLD. While there are many well-established techniques for force control, the application of force control to the human fingerpad in the literature is limited. Several researchers such as [12, 4, 3] have used single-axis actuators/indentors for applying normal force only to the fingerpad for the purpose of studying finger dynamics, while [5] used a single-axis actuator for applying shear forces only in order to study friction. Even in these cases, the actuators were controlled by position rather than force, with the force being simply a measured output. Bergamasco et al. [8] developed a high performance 3-axis force controller for a haptic device to apply 3-axis forces to the fingertip, where the fingertip is placed in a thimble. However the use of a thimble is a totally different situation, as it simply applies lumped forces to the entire fingertip and there are no distinct shear forces being controlled. To our knowledge, no one to date in the literature has attempted to perform simultaneous 3-axis force control on the surface of the fingerpad itself, controlling both normal and shear forces. Dynamic behavior of the fingerpad and coupling of the forces in the three axes due to the geometry of the fingerpad surface and frictional constraints make this a unique application.

In Section 2, this paper introduces our experimental system including the magnetic levitation device and finger restraint. In Section 3 the design, implementation and experimental validation of a three-axis force control method is described. In Section 4, the successful tracking of force trajectories for calibration of the fingernail imaging system is demonstrated.

2 Calibration Setup

To fully control all 3 directions of forces, a calibration platform is built on top of a magnetically levitated device (MLD) [1, 2] for automated calibration (Figure 1). The MLD uses an array of 6 Lorentz actuator coils within the spherical housing to levitate the flotor in the center. The flotor has a spherical workspace of radius ± 12 mm and $\pm 8^\circ$ 3-DOF rotation, and can produce 20 N of 3-D force and 4 Nm of 3-D torque. The motion and force/torque ranges are suitable for applying displacements and forces to the fingerpad in the range necessary to calibrate the fingernail imaging system, and is incapable of applying forces large enough to hurt the finger. The MLD also has advantages of high fidelity ($< 2\mu$m resolution) and high bandwidth (130 Hz) [1, 17], which should allow for excellent static and dynamic characterization of the force/coloration relationship.

To apply the MLD for calibration purposes, a 6-axis ATI Nano 17 force/torque sensor is attached the the flotor, which serves as the end-effector. A rubber-surface flat plane is mounted on the ATI Nano 17 force sensor to provide a flat contact surface with sufficient friction for the fingerpad. A Point Grey Flea video camera is mounted above the fingernail.

To provide a system in which the test subject is completely passive during the experiments, a method of restraining the motion of the finger is required. This finger restraint needs to allow the camera a clear view of the fingernail and surrounding skin. It must also restrict motion in all three directions so that the fingernail is in view of the stationary camera and the size of the fingernail image is approximately the same from one image to the next. As we plan to adjust the finger joint angle in later experiments, it is desired that the joint angle be controllable in some fashion. Previous research has established that the metacarpal phalangeal joint angle has no bearing on the finger coloration. We have thus far been unable to

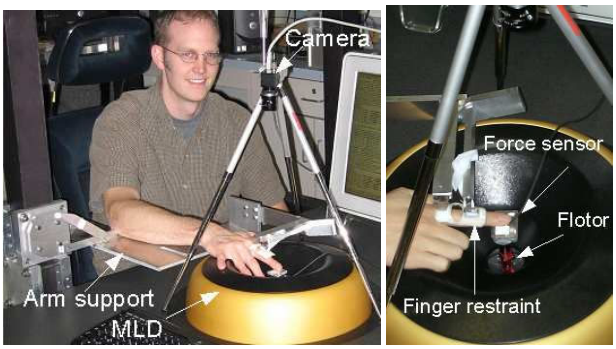

Figure 1: A calibration platform based on a MLD. A Point Grey Flea 2D high-resolution camera images a contact plane mounted on a 6-axis ATI Nano 17 force sensor and the MLD.

devise a method controlling the angle of the distal interphalangeal joint that does not obstruct the view of the fingernail and surrounding skin or affect the hemodynamics of the region we wish to image. The joint we intend to control, then, is the proximal interphalangeal joint, the middle joint on each finger. Additionally, the restraint should not affect the blood flow into the finger.

To accomplish these objectives, we chose to use a Roylan Static Progressive Finger Flexion Splint. We modified the splint as follows. First, we removed the section of the splint at the distal end of the finger. We also removed the screws for adjusting the angle of the finger joints. We attached the metal supports at the top to a linkage whereby we are now able to manually adjust the finger joint angle while holding the support in place. The splint includes straps to hold the finger in place on the restraint; however, tests showed that these straps alter the blood flow into the finger, so we removed these straps for our tests. The curvature of the plastic restraints hold the finger in place horizontally and prevent it from moving up. The pressure from the end effector prevents the finger from moving down. Thus, the finger is effectively restrained in all directions.

To hold the finger restraint in place relative to the MLD, an armrest was designed which attaches to the frame holding the chair. This armrest utilizes twin 4-bar linkages to allow the armrest to be lifted up and out of the way while a test subject positions themselves in the chair. A subject sits in a chair adjustable with 4 DOF for positioning relative to the experimental stage.

The MLD is controlled and operated by two PC based systems that communicate with each other using TCP/IP protocol through an Ethernet connection. The server PC (operating on QNX) directly controls the Lorentz actuators within the MLD using feedback from optical position sensors, while the client PC (operating on Ubuntu) run the user interface and sends desired position commands to the server.

The server is designed to run a PID position controller with gravity compensation. Therefore, the client must currently be used to implement force control as a separate outer loop, while the server implements position control on an inner loop, both running at 1 kHz with parallel timers. Forces are measured by the ATI Nano 17 force sensor. The force measurements are filtered with an ATI signal conditioning and amplification box and read using the A/D inputs on a Sensoray 626 data acquisition board installed in the client PC. The force controller on the client uses the force feedback to send desired position commands to the server. The client also runs another process to drive the Point Grey Flea video camera to capture images at 30 fps and synchronously record forces. To optimize speed, the network communications are kept to a minimum, where the desired position is the only communication between the client and server.

3 CONTROL CONTROL

3.1 Control Objectives

For the purposes of this paper and future research involving fingernail imaging, we desire to control the force applied to the finger pad in three directions. Our objectives in this control scheme are: (1) minimize the force error; (2) minimize the duration of the calibration tests; and (3) ensure stability of the controller.

The first requirement, minimizing the force error, is dependent both on the density with which we wish to cover the force workspace and the accuracy/precision of the force sensor. The workspace we wish to cover is detailed in Section 4 on Trajectory Design. Briefly, we wish to apply forces in intervals of 0.1 Newtons in each of the three force directions over the range of interest. This range is 0-10N of normal force and $+/-5$N of shear. We therefore want to achieve a steady-state force error less than 0.05 Newtons in each of the three force directions. This is due to our findings in [16], where we learned that our imaging method is able to distinguish between force levels up to 0.1 Newtons. The force sensor has a resolution of less than 1 mN in each direction, and an RMS noise level of 0.03 Newtons. Thus, we should be able to keep the force error within the specified limit using integral force control.

The second requirement, minimizing the duration of the calibration tests, is limited by the speed with which our controller tracks the desired force and the speed of the dynamics of the color change of the fingertip. The hemodynamics of the fingertip have been shown to have a time constant of approximately 0.1 seconds [14]. Therefore, the time constant of the force controller should be at least as fast to minimize calibration time.

Stability, our third requirement, is vital to these experiments. At worst, instability in our controller could damage the MLD. At best, momentary instability typically results in the flotor oscillating out of its operational workspace, which requires a separate utility to be run to reset the flotor before resuming normal operation. The gain and phase margins of our controller will be examined to ensure that the controller will remain stable for a wide range of gains.

3.2 Control Design

Feedback force control of the MLD has not been studied in much detail. The MLD API is primarily designed to support closed-loop position control on the server PC. It also allows the client to specify a desired force, but the server does not accept force feedback and only uses open-loop commands on the Lorentz coils to attempt to achieve the desired force. The large force errors present in this method makes it unsuitable for our application. Therefore, we have designed our own closed-loop force controller for the MLD that runs on the client PC.

We considered two possibilities for our force controller on the client: (1) a direct force controller with computed torque control or (2) a force controller with an inner position loop, as in [13]. For the first case, we would directly control the six coil currents in the MLD. In the second case, we would utilize the existing (and very accurate) PD position controller of the MLD.

Direct force control is possible, as the MLD API does allow the client to send commands for the six Lorentz coil currents, however the coupled dynamics of the coils and flotor have not yet been provided. Additionally, use of the position controller as an inner loop has the advantage that we are specifying a desired position at each iteration of the control loop. Thus, we can verify that we are not commanding the flotor to move outside the workspace boundary, necessitating a resetting of the flotor. Therefore we have chosen to use a force controller with an inner position loop. The controller block diagram is shown in Figure 2.

The inner position loop is controlled completely by the MLD server. We set the controller gains K_D and K_P before beginning the control process and then supply the desired position X_d. The integral gain on the inner loop is set to zero since the outer force loop has its own integral control to ensure the desired force is achieved.

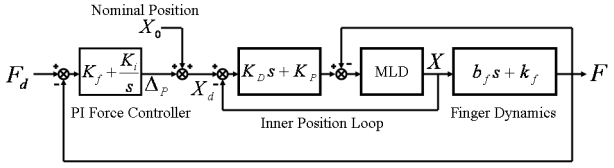

Figure 2: Block diagram of force controller showing inner position loop and outer force loop. There is also a loop illustrating the reaction force of the finger acting back onto the MLD.

The finger dynamics represent the stiffness and damping effect of the force sensor interacting with the finger pad. Although these dynamics are nonlinear [7], we have chosen to model the dynamics as a linear approximation, since our range of forces is small. In order to simulate the system, we have estimated the finger stiffness kf as $1200N/m$ and the finger damping bf as $5N/(m/s)$. Eventually, we intend to use the controlled system to verify the nonlinear characteristics of the fingerpad. However, our intent at this point is to design a controller with a gain margin such that the controller will be stable for a range of stiffness and damping parameters.

A PI force controller is implemented on the client as $\Delta_p = K_f(F_d - F) + K_i \int (F_d - F)dt$. The nominal position X_0 represents the desired nominal position at which the force will be applied. The desired position is calculated as: $X_d = X_0 + \Delta_p$ and sent to the server.

There is no derivative gain on the force controller since the force feedback is noisy and should not be differentiated. If more damping is required to stabilize the system, the derivative gain on the position controller can be increased.

Since the MLD position controller decouples the control of the three axes, the design of the controller is simplified. The inner (position) loop gains are adjusted so that each of the three axes can be approximated by the same second-order system. Thus, our controller can be duplicated in each of the three axes. Figure 3 illustrates the implementation of the controller. The lowest right box represents the server, the computer implementing the MLD position controller. The upper left box represents the client, the computer implementing our force controller and handling all of the data output. The desired position X_d is transmitted to the server across the Ethernet connection at each iteration of the control loop. The position controller moves the flotor to the desired position, causing the force applied by the flotor to the finger to change. This is detected by the force sensor and read by the client. The client reads the force sensor and outputs a desired position.

To design the gains for the force control loop, K_f and K_i, root locus methods were used. The MLD with PD position control (inner loop) was modeled as a second-order system with one zero at $-K_p/K_d$. In order to determine the closed loop poles of the inner position loop, a step input of 1 mm was sent to the position-controlled MLD and the rise time (0.5 s) and percent overshoot (50%) were measured. The closed loop poles from the inner loop then become open loop poles for the outer loop. The finger dynamics add one zero at $-k_f/b_f$. The force controller adds a pole at the origin and a zero at K_i/K_f. The root locus of the complete open-loop system is shown in Figure 4. (The zero at $-K_i/K_f$ is not shown as it is very large.) The root locus indicates that the system should be stable for a wide range of gains. Although desirable gains could be chosen directly from the root locus, in practice, better results were obtained by experimental gain tuning due to uncertainty in the finger dynamics and the presence of other unmodeled dynamics. Experimentally, it was found that $K_i = 200$ m· s/N and $K_f = 0.001$ m/N resulted in optimal performance for all three axes.

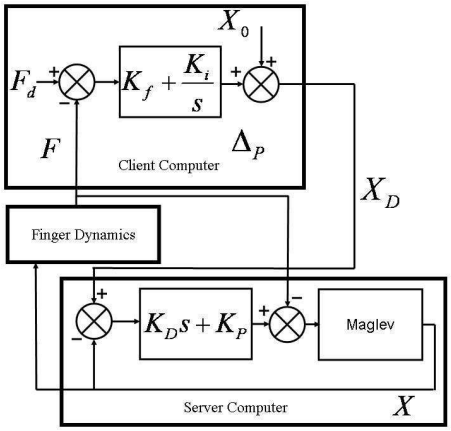

Figure 3: Schematic of client-server communication and implementation of the control loop.

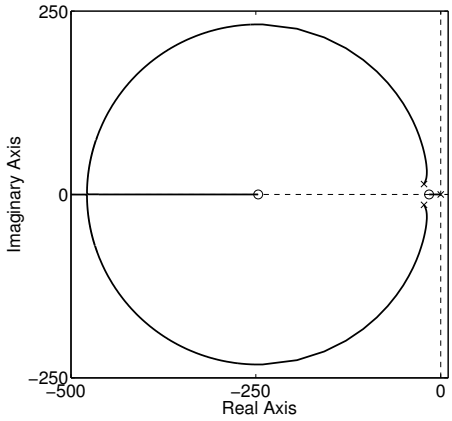

Figure 4: Root locus of the force controller

3.2.1 Experimental Results

To test the implementation of the controller as designed, a step input of 1 N desired force was applied in turn to each of the three principal force directions. The response for the y-direction is shown in Figure 5. The responses of the x and z directions are at least as fast, with rise times of approximately 0.1 second in each axis. Figure 4 also shows good disturbance rejection by the x- and z-axis controllers in response to a step in y.

The step input was then applied to all three directions at once. The results are shown in Figure 6. Note that the step in Z is negative because force increases in the negative Z direction. The response is stable and settles in approximately 0.2 seconds.

Another test was the implementation of a circular force trajectory with frequency $\omega = 1$ rad/s. The results are shown in Figure 7. The x-direction force tracks with an RMS error of 0.08 N, while the y-direction force tracks with an RMS error of 0.17 N. (For reference, all three directions have a steady-state RMS error of approximately 0.05 N when holding a constant value.)

To calculate the gain and phase margins, sinusoidal inputs were applied to the force controller at varying frequencies between 0.01 and 100 Hz. The frequency response was measured and a Bode plots for the x- and z-directions are shown in Figure 8. The y-direction plot is similar to the z-direction. The gain margin was found to be approximately 2.2 in the x-direction, 6.3 in the y-direction and 3.1 in the z-direction. This result indicates that the controller has some margin of stability but may have trouble if there are large variations in finger dynamics. There is no primary resonance peak on either plot, indicating that the systems are overdamped. The x-direction Bode plot shows a resonance peak at 30 Hz, indicating the presence of unmodeled dynamics, which limits the gain margin. This may be due to a larger compliance in the finger restraint in the x-direction than the other two. If the source of these unmodeled dynamics can be identified in future work, perhaps the gain margin can be improved. The y- and z-directions show no such peak.

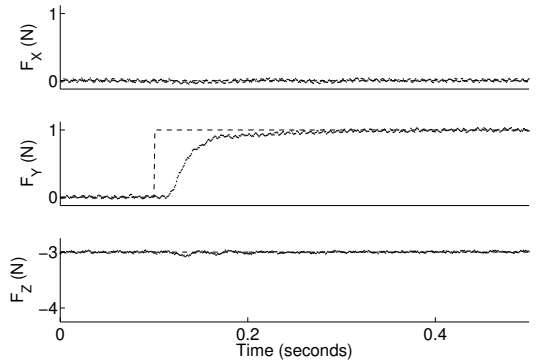

Figure 5: Y-direction force step response. The desired force trajectory is shown as dashed lines and the measured force on the finger pad is shown as solid lines.

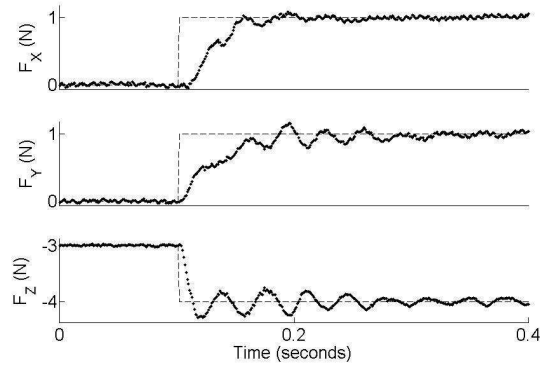

Figure 6: 3-direction force step response. The desired force trajectory is shown as dashed lines and the measured force on the finger pad is shown as solid lines.

A final observation is that the stability of the force control is dependent on operating within acceptable ratios of shear force to normal force, as defined by the coefficient of friction between the finger and the end-effector. If the desired shear force becomes too large, there will not be enough friction to achieve it, and the control will destabilize. In practice, the end-effector quickly oscillates outside of the designed workspace and requires resetting. This requires placing proper limits during trajectory design to avoid unstable combinations of desired forces.

4 Force Trajectory Design

For the fingernail imaging system, a desired force trajectory must be created to generate a rich set of training data that will be used to calibrate the model relating forces to fingernail coloration. The feasible force space is a 3-D cone defined by the constraints of max-

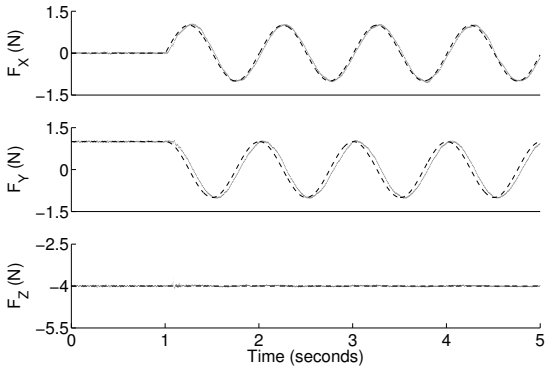

Figure 7: Circular force trajectory tracking. The desired force trajectory is shown as dashed lines and the measured force on the finger pad is shown as solid lines.

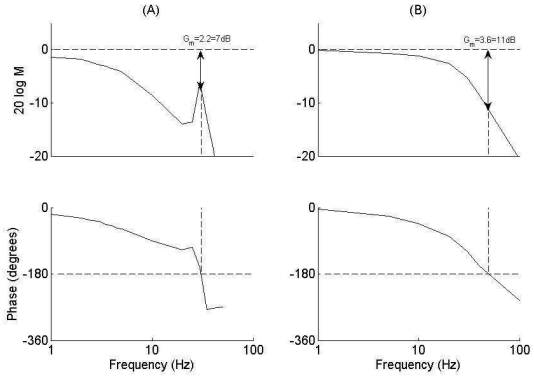

Figure 8: Bode plots for (A) the x-direction and (B) the z-direction. The y-direction plot is similar to that of the z-direction. The gain margin for the x-, y- and z-directions are 2.2, 6.3 and 3.1, respectively.

imum normal force and frictional shear force, as depicted in Figure 9.

Due to the frictional constraint, the range of possible shear force magnitudes increases linearly with normal force. However, the training data should be spread uniformly across the cone space in order to create a model that is not biased toward any specific portion of the space (unless a specific application suggests otherwise).

The training data can be specified to be of uniform density in either cylindrical coordinates or Cartesian coordinates. If cylindrical coordinates are chosen, the model will be unbiased in terms of magnitude and direction of shear force; whereas, if Cartesian coordinates are chosen, the model will be unbiased in terms of the magnitudes of the individual shear force components. Depending on the application of the fingernail imaging system, either method may be preferable. In either case, the training data should be uniform in magnitude of normal force.

It takes a relatively long time (30 ms) to take an image for our 30 fps video camera. Therefore the force trajectory should be designed to move from waypoint to waypoint in the force space, wait at least 0.1 seconds for the force and fingernail coloration to settle, and then wait another 30 ms for the image acquisition before moving to the next waypoint. To limit the duration of the calibration, only a certain number of waypoints in the cone-shaped force space are selected for calibration. A trajectory that connects all the waypoints is generated by directly connecting adjacent waypoints. At each waypoint, the force controller controls the MLD to keep the force

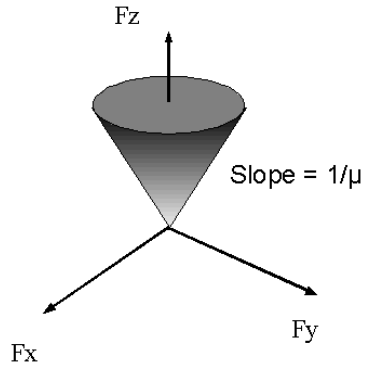

Figure 9: 3D cone-shape force space

for at least 0.2 seconds for the camera to take the recording.

In a Cartesian coordinate system, the cone-shape force space is latticed with a 3-D grid to generate waypoints. Figure 10 shows a force trajectory generated in a Cartesian coordinate system.

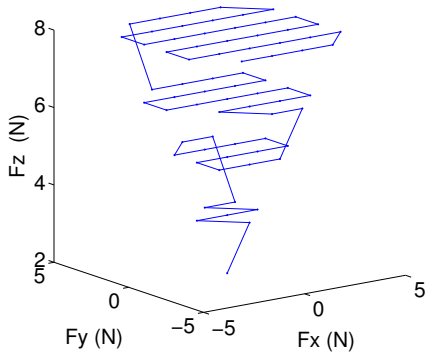

Figure 10: A force trajectory generated in a Cartesian coordinate system.

In order to create a set of training data with a uniform cylindrical density, the cone-shape force space is latticed in normal force, shear force magnitude, and shear force direction. An Archimedean spiral [6] is used to connect all the waypoints in a cylindrical coordinate system, as shown in Figure 11. At each normal force level, in polar coordinates (r, θ) the relation between radial and angle can be described by the equation $r = b\theta$, while b controls the distance between successive turnings of the spiral.

The next step was to input a trajectory similar to those we plan to use in our fingernail imaging calibration experiments. We chose to use a trajectory composed of Cartesian grid sampling in the cone-shaped region with a step size of 0.1 N in all three directions. The trajectory contains 152 calibration points. We chose to ramp up to each point in 0.1 seconds and hold the data point for 0.4 seconds, for a total time of 76 seconds. Figure 12 shows a trajectory tracking result. As can be seen from the figure, the actual forces follow the desired forces very closely. The RMS error was calculated for these tests and found to be 0.07 N in the x-direction, 0.06 N in the y-direction and 0.05 N in the z-direction. These errors are all within the specified goals for our force tracking and meet the needs of the fingernail imaging calibration.

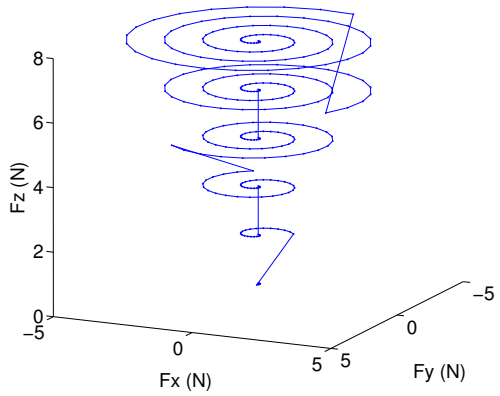

Figure 11: 3-D force trajectory based on Archimedean spiral.

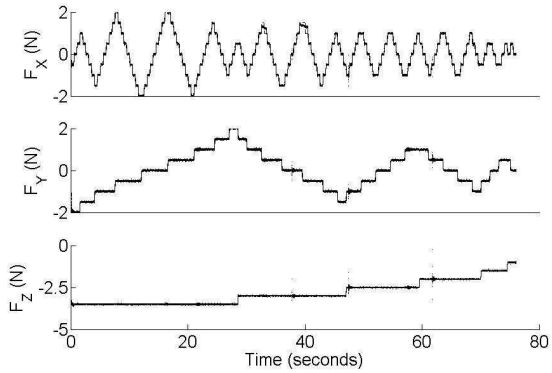

Figure 12: Force trajectory tracking. The desired force trajectory is shown as dashed lines and the measured force on the finger pad is shown as solid lines.

5 Conclusion

In summary, this paper demonstrated successful three-axis force control when a flat surface is pressed against the human fingerpad using a 6 DOF magnetic levitation device. The system is capable of taking simultaneous steps in normal force and two axes of shear forces with a settling time of less than 0.2 seconds, and achieves a steady-state error as small as 0.05 N in all three axes due to the integral action of the force control. The system is also capable of tracking error of less than 0.2 N when the shear force vector rotates with a frequency of 1 rad/s. The primary application of this force control is for the automated calibration of a fingernail imaging system, where video images of the human fingernail are used to predict the normal and shear forces that occur when the fingerpad is pressed against a flat surface. This paper demonstrated the successful tracking of a desired force trajectory for generating training data necessary for calibrating the fingernail imaging system. This work could also find other applications in using the MLD to provide haptic feedback to the fingerpad for human-computer interaction and virtual reality. The MLD itself is an ideal platform for performing 3-axis force control due its highly responsive direct-drive dynamics and inherent inability to harm the fingers.

In future work, the authors would like to also automate the variation of the contact angles of the fingerpad with the surface, and possibly also add a shearing torque about the z-axis. Although the MLD flotor itself has three rotational degrees of freedom that can be controlled, the angular range of motion is too small to be of use in this application. Therefore the authors plan to augment the MLD with two or three additional degrees of freedom for varying the roll, pitch, and yaw on a larger scale. The final system would then have simultaneous 3 DOF force control along xyz, 1 DOF torque control about z, and 2 DOF angular position control about x and y.

Acknowledgements

This work was supported by NIH Grant 1R21EB004600-01A2. We thank Dr. Ralph Hollis, Kei Usui, and Hanns Tappeiner at CMU for their help and support of setting up the MLD system.

References

[1] P. Berkelman and R. Hollis. Lorentz magnetic levitation for haptic interaction: device design, function, and integration with simulated environments. *Intl J Robotics Research*, 9:644–667, 2000.

[2] CMU. *Magnetic Levitation Haptic Interface User Manual*, 2008.

[3] R. Gulati and M. Srinivasan. Human fingerpad under indentation i: Static and dynamic force response. In *ASME Bioengineering Conference*, volume 29, pages 261– 262, 1995.

[4] H. Han and S. Kawamura. Analysis of stiffness of human fingertip and comparison with artificial fingers. In *Proceedings of the IEEE Conference on Systems, Man, and Cybernetics*, pages 800–805, 1999.

[5] H. Han, A. Shimada, and S. Kawamura. Analysis of friction on human fingers and design of artificial fingers. In *Proceedings of the IEEE International Conference on Robotics and Automation*, pages 3061–3066, 1996.

[6] J. D. Lawrence. *A Catalog of Special Plane Curves*. New York: Dover, 1972.

[7] J. Liao and M. A. Srinivasan. Experimental investigation of frictional properties of the huamn fingerpad. Technical report, MIT, Touch Lab, 1999.

[8] S. Marcheschi, F. Salsedo, M. Fontana, F. Tarri, O. Portillo-Rodriguez, and M. Bergamasco. High performance explicit force control for finger interaction haptic interface. In *World Haptics*, pages 464 – 469, 2007.

[9] S. Mascaro and H. Asada. Photoplethysmograph fingernail sensors for measuring finger forces without haptic obstruction. *IEEE Transactions on Robotics and Automation*, 17(5):698–708, 2001.

[10] S. Mascaro and H. Asada. The common patterns of blood perfusion in the fingernail bed subject to fingertip touch force and finger posture. *Haptics-e: The Electronic Journal of Haptics Research*, 4(3):1–6, 2006.

[11] S. Mascaro and H. H. Asada. Measurement of finger posture and three-axis fingertip touch force using fingernail sensors. *IEEE Trans. on Robotics and Automation*, 20:26–35, 2004.

[12] D. Pawluk and R. Howe. Dynamic contact of the human fingerpad against a flat surface. *Journal of Biomechanical Engineering*, 121(6):605–611, 1999.

[13] Sciavicco and Siciliano. *Modeling and Control of Robot Manipulators*. London; New York: Springer, 2000.

[14] Y. Sun, J. M. Hollerbach, and S. A. Mascaro. Dynamic features and prediction model for imaging the fingernail to measure fingertip forces. In *Proc. IEEE Intl. Conf. Robotics and Automation*, pages 2813–2818, 2006.

[15] Y. Sun, J. M. Hollerbach, and S. A. Mascaro. Measuring fingertip forces by imaging the fingernail. In *Proc. 14th Symposium on Haptic Interfaces for Virtual Environment and Teleoperator Systems*, pages 125–131, 2006.

[16] Y. Sun, J. M. Hollerbach, and S. A. Mascaro. Predicting fingertip forces by imaging coloration changes in the fingernail and surrounding skin. *IEEE Trans. on Biomedical Engineering*, 55(10):2363–2371, 2008.

[17] B. J. Unger, R. L. Klatzky, and R. L. Hollis. Teleoperation mediated through magnetic levitation: Recent results. In *IEEE Conf. on Mechatronics and Robotics*, pages 1453–1457, 2004.